Functional Materials 13, No.3 (2006)

The structure and crystallisation of laser condensates of vanadium deposited in oxygen atmosphere

A.G.Bagmut, S.N.Grigorov, V.A.Zhuchkov, V.Yu.Kolosov, V.M.Kosevich, D.V.Melnichenko*

National Technical University "Kharkiv Polytechnic of Institute",
21 Frunze St., 61002 Kharkiv, Ukraine
*Ural State Economic University, 62 8th March St.,
620026 Ekaterinburg, Russia

The phase composition and structure of films deposited by laser sputtering of V in oxygen atmosphere have been diagnosed by electron diffraction and transmission electron microscopy using "in situ" procedures as well as by consideration of bend extinction contours. It has been shown that at the substrate temperature T_s ranging from 20 to 360°C and the oxygen pressure $P(O_2)$ in the evaporation chamber from $5 \cdot 10^{-3}$ to $1.3 \cdot 10^{-1}$ Pa, the oxygen concentration in the film increases as the $P(O_2)$ rises at fixed T_s, while at fixed $P(O_2)$, it decreases as T_s is elevated. The existence areas and compositions of the crystalline ($VO_{0.9}$) and amorphous (V_2O_3) phases have been established as well as the fact of the film composition fractionation as a function of the vapor-plasma flow condensation angle. The V_2O_3 spherulites growing in the amorphous phase have distorted (bent) crystal lattice, the bend attaining about 42 deg per μm. The amorphous phase crystallization is accompanied by the density increase by 9.2 %.

Методами электронографии и просвечивающей электронной микроскопии с использованием методик "in situ" и анализа изгибных экстинкционных контуров диагностированы фазовый состав и структура пленок, осажденных лазерным распылением V в атмосфере кислорода. Показано, что в интервале температур подложки T_n (20–360°C) и давлений кислорода в испарительной камере $P(O_2)$ ($5 \cdot 10^{-3}$–$1.3 \cdot 10^{-1}$ Па) при фиксированной T_n содержание кислорода в пленках возрастает с увеличением $P(O_2)$, а при фиксированном $P(O_2)$ оно уменьшается с ростом T_n. Установлены области существования и состав кристаллической ($VO_{0,9}$) и аморфной (V_2O_3) фаз, а также эффект фракционирования состава пленки по углу конденсации паро-плазменного потока. Сферолиты V_2O_3, растущие в аморфной пленке, имеют искривленную кристаллическую решетку. Величина искривления достигает ~42°/мкм. Кристаллизация аморфной фазы V_2O_3 сопровождается увеличением плотности на 9,2 %.

The materials in amorphous thin-film state are effective precursors for synthesis of nanostructure materials. In this respect, the amorphous oxygen-containing films prepared by pulse laser sputtering of metals in oxygen atmosphere, are of good prospects. By varying the ratio of metal and gas flows to the growing surface of a film, a wide variety of structural and phase conditions is possible to obtain ranging from crystal metal up to amorphous oxide. By post-condensation heat treatment of amorphous film, it is possible to realize a predominant, polymorph or eutectic type of crystallization, depending on the deviation degree of the film composition from stoichiometry [1]. The film composition deviation from stoichiometry influences also on the crystal lattice bending degree of spherulites being, formed in amorphous films [2]. In V–O system, more than 11 compounds of vanadium with oxygen have been found [3]. One of

those, vanadium dioxide (VO_2), was obtained also by laser evaporation of metal in oxygen atmosphere [4, 5]. Yet the literary data concerning structural diagnostics (using electron diffraction and electron microscopy methods) of phase formation in the V–O system, are absent as far as we know. The purpose of this work is to study the influence of the substrate temperature T_s and of the oxygen pressure $P(O_2)$ in the evaporation chamber on the structure and phase composition of laser condensates of vanadium using the electron diffraction and electron microscopy investigation as well as to study the features of the amorphous-crystal phase transition as a result of the film heat treatment.

The films were prepared on KCl substrates ((001) orientation) by a standard laser deposition technology [2, 6] using the pulse sputtering of a high purity vanadium target in oxygen atmosphere in a flow-through mode. The film thickness t was 25 to 30 nm. Nanosecond laser pulses at the 1.06 μm wavelength in the Q-switch mode were used. The pulse repetition frequency $\nu = 25$ s^{-1}. The substrate temperature T_s was varied from 20 up to 360°C. The oxygen pressure in the evaporation chamber $P(O_2)$ was varied from $5\cdot10^{-3}$ up to $1.3\cdot10^{-1}$ Pa; the condensation angle β of the laser erosion plasma (to the normal to the substrate surface) was varied from 9 to 28°. The film structure was investigated by the transmission electron diffraction and electron microscopy using the analysis of bend extinction contours technique [7] and measurements of the relative density changes η of the film substance at the amorphous to crystal state transition [6]. It is known that the crystal lattice of spherulite growing in amorphous matrix is regularly curved [7]. The local specific angle of the crystal lattice turning θ_{loc} characterizes such a curvature. It describes the rotation of crystal planes per unit length of a crystal and is expressed in deg/μm. It was determined using zone-axle pictures of bend extinction contours in the electron-microscopic images of crystals according to the relationship

$$\theta_{loc} = \frac{360}{\pi W}\arcsin\left(\frac{\lambda}{2d_{hkl}}\right), \qquad (1)$$

where W is the distance between pair of bend extinction contours corresponding to diffraction vectors $\mathbf{g}_{hkl}$ and $\mathbf{g}_{\overline{hkl}}$; d_{hkl}, the interplanar distance; λ, the electron wavelength. The specific integral angle of crystal lattice turning Θ_{int} was determined as:

$$\Theta_{\text{int}} = \frac{\varphi}{L}, \qquad (2)$$

where L is the distance between the centers of zone-axle pictures with zone axes directed to $[u_1v_1w_1]$ and $[u_2v_2w_2]$; φ, the angle between these zone axes.

The relative density change η, accompanying the crystallization, was determined as:

$$\eta = \frac{\Delta\rho}{\rho} = \left(\frac{X_A}{X_C}\right)^3 - 1. \qquad (3)$$

In Eq.(3), $\Delta\rho = \rho_C - \rho_A$, where ρ_A and ρ_C are the material density values in amorphous and crystal state, respectively; X_A and X_C, the distances between fixed labels on the same site of a film before and after crystallization. As the labels fixed to the film, the solidified micro droplets of melt usually observed at laser sputtering of a metal ("spray" effect) were used.

The following results of electron-microscopic investigations of the substrate temperature T_S and the oxygen pressure in the evaporation chamber $P(O_2)$ effects on the film structure and phase composition have been found. It has been established that at fixed T_S, the oxygen content in the films increases as $P(O_2)$ rises, while at fixed $P(O_2)$ it decreases with increasing T_S. At $P(O_2)$ of $5\cdot10^{-3}$ Pa, in the T_S interval from 20 up to 360°C the film of $VO_{0.9}$ composition is formed on (001) KCl substrates at laser sputtering of V target. All reflections of the diffraction patterns presented in Fig. 1 correspond to this compound $VO_{0.9}$ in accordance with data of the card file No.10–0313 [8] (vanadium oxide $VO_{0.9}$; fcc lattice with parameter $a_0 = 0.412$ nm). At $T_S = 20$°C, a polycrystal film (Fig. 1a) is formed. Above 190°C (Fig. 1b), the $VO_{0.9}$ film grows at predominant orientation according to the relation

$$(001) < 110 > VO_{0.9} // (001) < 110 > KCl. \qquad (4)$$

At the same time, the presence of {111} reflections in the diffraction pattern and of a primary diffraction on twins (marked as DD) [9] indicates that for some grains of $VO_{0.9}$, the following orientation relationship takes place:

$$(111) < 110 > VO_{0.9} // (001) < 110 > KCl. \qquad (5)$$

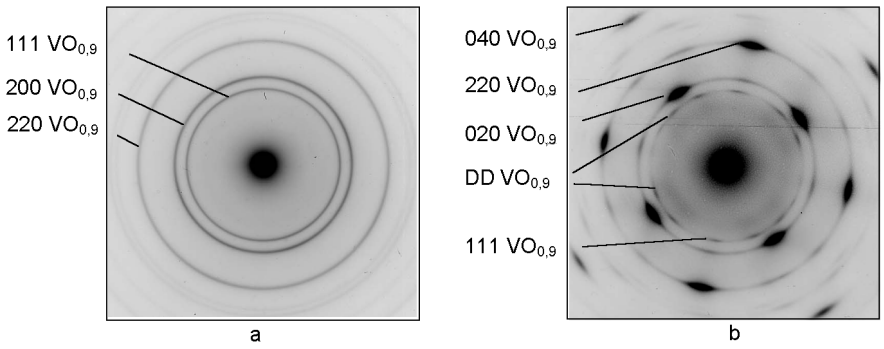

Fig. 1. Electron diffraction pictures of films deposited at laser sputtering of V on substrates (001) KCl at $P(O_2) = 5 \cdot 10^{-3}$ Pa: $T_s = 20$°C (a); $T_S = 360$°C (b).

The relations (4) and (5) are typical of the epitaxial growth of metals films with fcc structure (for example Au) at condensation on (001) surfaces of alkali halide crystals [10]. At $P(O_2) = 1.3 \cdot 10^{-1}$ Pa within the T_s interval from 20 up to 200°C, the condensates with amorphous (V_2O_3) and crystal ($VO_{0.9}$) components are formed. The amount of fine-dispersed crystal $VO_{0.9}$ phase in the films increases with elevating substrate temperature T_s, thus corresponding to the general increasing of V content in the film. This is in agreement with the general trend to decreasing efficiency of oxygen capture in the growing film at increasing T_s at fixed $P(O_2)$ [2].

The effect of phase composition fractionation in the film depending on the condensation angle β of the plasma-vapor flow has been revealed. The $VO_{0.9}$ crystal phase content in the laser condensates decreases with increasing β (the angle β being measured from the normal to the substrate surface). The structure and phase composition of films deposited at β = 10°C is illustrated by Figs. 2a and 2b. In the initial state, the film is biphase: both amorphous and crystal ($VO_{0.9}$) phases are present. After the film heating with electron beam, the amorphous phase is crystallized with formation of V_2O_3 spherulites. At β ≅ 19°C, the $VO_{0.9}$ crystal phase has been not revealed by electron diffraction and microscopy. An amorphous single-phase condensate is formed (Figs. 2c, 2d). After the film crystallization by means of electron beam, its composition corresponds to V_2O_3 (Fig. 2f). All reflections in this diffraction pattern belong to V_2O_3 and are in accordance with data of the card file No.26-0278 [11] (vanadium oxide V_2O_3; rhombohedral lattice with parameters $a = 0.4920$ nm, $c = 1.3883$ nm and $c/a = 2.8217$).

Thus, with the reduction of β, the total content of vanadium in the films increases, while the oxygen one decreases. Qualitatively, this is in agreement with the character of angular distribution of laser erosion plasma particles. For example, the angular distribution diagrams of neutral Co atoms under laser radiation with the similar characteristics are "extended" along the normal to the sample [12]. This results in an improvement of so-called "effective" vacuum (i.e. to the reduction of oxygen "effective" pressure) [13] near the propagation axis of the vapor-plasma flow. A flow of metal vapor and plasma ejects oxygen from the propagation axis to the periphery. It is natural that in this case, the oxygen concentration in films increases with enlarging condensation angle β of laser erosion plasma. The stability of amorphous component in laser condensates of vanadium was investigated under annealing of the prepared films on the substrate. The annealing was realized in vacuum after pumping-out of oxygen without the re-pressurization of the evaporation chamber. At annealing temperatures $T_{an} \leq 450$°C, no crystallization of amorphous component was observed.

The amorphous films crystallize under electron beam heating. At the initial stage of transformation, three primary morphological types of V_2O_3 crystals have been observed. The rounded form crystals are oriented so that the basic plane (001) of V_2O_3 is parallel to the film surface. As to strip-like and crescent-shaped crystals, various crystallographic planes may be parallel to the film surface. The same three primary morphological forms were observed before for Cr_2O_3 crystals (having

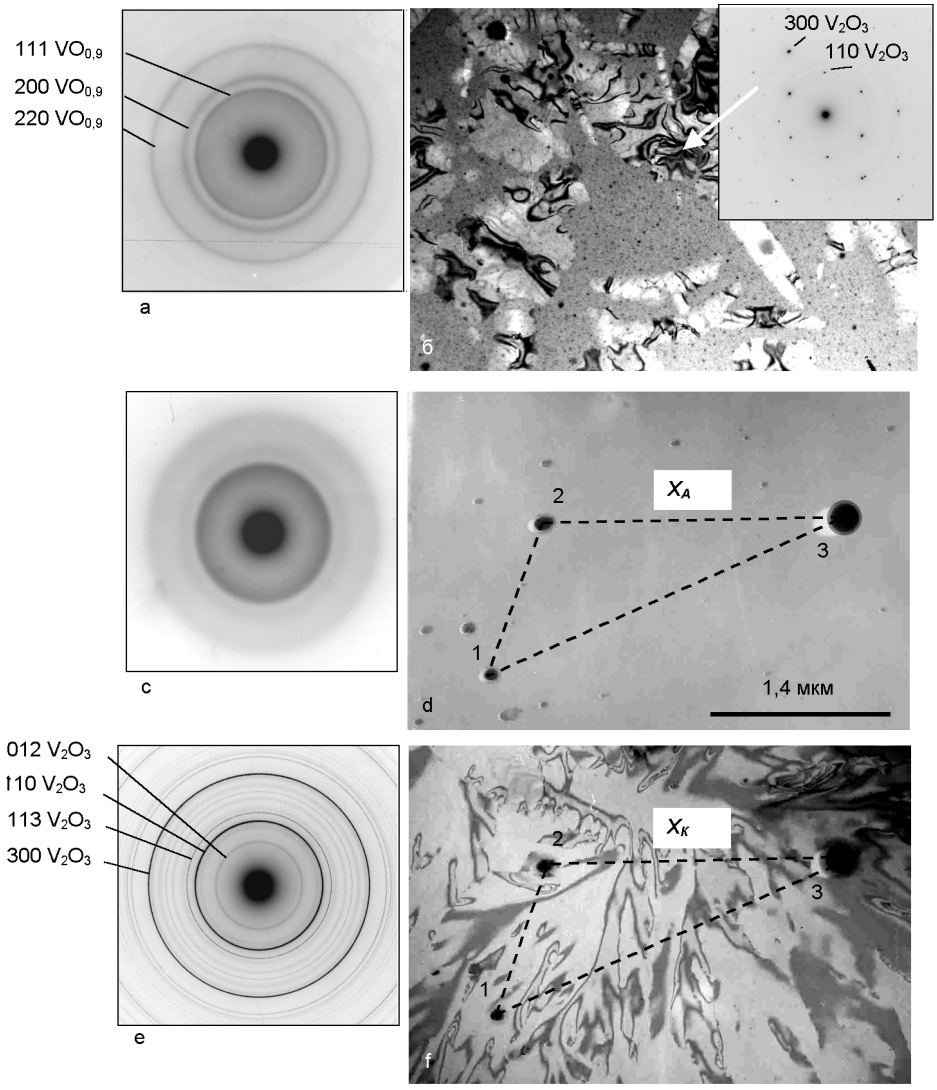

Fig. 2. The structure of films deposited at laser sputtering of V at T_s = 20°C in oxygen atmosphere at $P(O_2) = 1.3 \cdot 10^{-1}$ Pa: electron diffraction picture from a two-phase film (crystal $VO_{0.9}$ and amorphous V_2O_3) in the initial state, the condensation angle of laser erosion plasma β = 10° C (a); micrograph of this film after its partial crystallization with electron beam (b), at the right top corner of the micrograph the electron diffraction pattern of a V_2O_3 spherulite is given; c, d condensation at β = 19° C; the electron diffraction pattern and micrograph of this film after its overall crystallization (e, f, respectively). The position of adjoined marks (microdrops of V) before and after crystallization of a film is indicated by a dotted line 1–2–3.

crystal lattice similar to that of V_2O_3) growing in amorphous films prepared in the same way by laser sputtering of Cr in oxygen atmosphere [6]. As a rule, the homogeneous nucleation of strip-like crystals takes place in amorphous matrix (the terminology used in [6] is kept). The crescent-shaped crystals are formed in the course of trans-rotational distortion of strip-like crystals. The rounded shape crystals can nucleate both in the free state and in a bound state-heterogeneously on a side surface of a strip-like or crescent-shaped crystal.

A typical example of morphology and orientation evolution of the crystals is shown in Fig. 3. First, a strip-like V_2O_3 crystal (area 1) is nucleated oriented so that the V_2O_3 plane (1 0 5) is parallel to the amorphous film surface. During the growth process the crystal lattice turns about an axis perpendicular to the $(\bar{1}\ 2\ 0)$ planes at the angle $\theta_{1,2} = 14.48°$ ($\theta_{1,2}$ being the angle between directions of zone axes [211] and

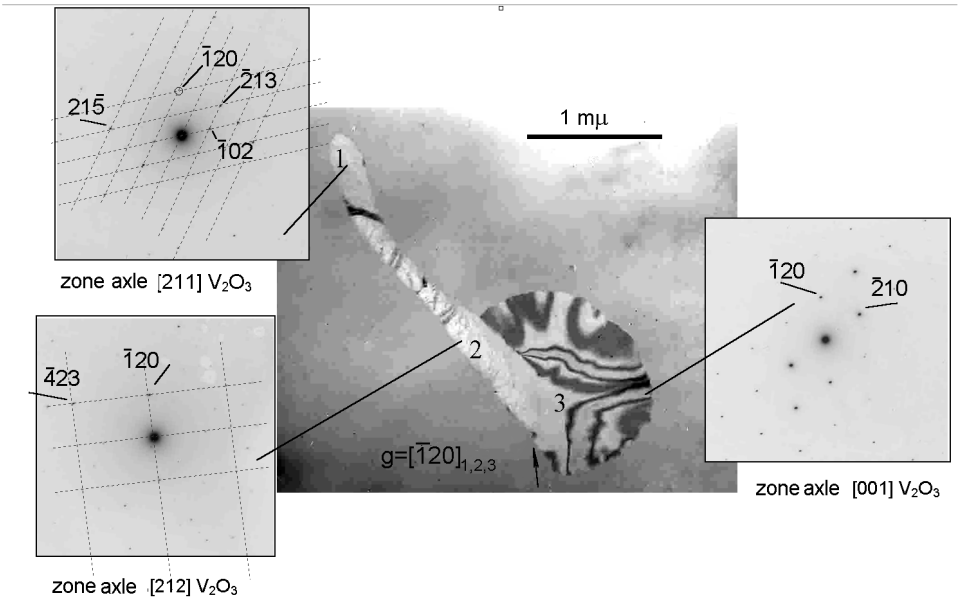

Fig. 3. The structure and morphology of V_2O_3 crystals growing at the electron beam heating of amorphous films in a column of an electron microscope. *1* and *2*, the different areas of the same strip-shaped crystal. *3*, the rounded crystal (the terminology used in [6] is kept). The reflections belonging to above-mentioned zones of crystal planes are connected with dashed lines (at two selected areas of diffraction patterns positioned in the left part of the micrograph).

[212] at areas 1 and 2 of the crystal). Then the rounded crystal 3 grows epitaxially at the side crystal surface in the area 2 as on a seed. The crystal lattice of a crystal 3 is rotated with respect to the area 2 at the angle $\theta_{2,3} = 17.06°$ ($\theta_{2,3}$ is the angle between directions of zone axes [212] and [001] of areas 2 and 3, respectively). The crystal 3 is oriented so that the V_2O_3 planes (0 0 1) are parallel to the amorphous film surface. As a rule, the crystals of this orientation have the rounded form, that is just observed in this case. The resulting rotation angle $\theta_{1,3} = 31.54°$ ($\theta_{1,3}$ being the angle between directions of zone axes [211] and [001] of areas 1 and 3, respectively). Accurate to two decimal places, $\theta_{1,3} = \theta_{1,2} + \theta_{2,3}$. In areas 1–2–3 of epitaxial joint V_2O_3 crystals, the following relation is valid:

$$(\bar{1}20)_1[211]_1//(\bar{1}20)_2[212]_2//(\bar{1}20)_3[001]_3, \quad (6)$$

where the planes ($\bar{1}$ 2 0) of V_2O_3 are perpendicular to the film surface and their orientation is the same in all three areas of the film (Fig. 3).

The crystallization of amorphous phase is accompanied by increasing film material density. The typical picture of a polymorph (i.e. at unchanged film composition) transition from amorphous to crystal state is shown in Figs. 2d and 2f. The broken dashed line 1–2–3 connects the conjugated labels, the distance between those being changed after the film crystallization. This makes it possible to measure the relative V_2O_3 density changes η accompanying the amorphous-to-crystal transition using expression (3). For example, the change of the distance between labels 2 and 3 in Fig. 2d is such that $X_A/X_C = 1.032$. According to (3), $\eta \approx 9.9$ %. The statistical processing of the numerical data obtained using a number of microphotos, the average value of η is about 9.2 %.

The positive value of η indicates the increasing density of the film material after its crystallization. Therefore, the V_2O_3 crystal nucleus growing in amorphous matrix is always subjected to tensile stress. As a result, the crystal bends in a regular fashion, as is seen in Fig. 4. In this figure, the straight lines denote the mutual unambiguous connection between reflections in the diffraction patterns and bend extinction contours in the microphotograph. The selected area diffraction pattern from the area 4 is related to a rounded crystal grown heterogeneously on a side surface of a strip-like one. The presence of a contrast bend extinction

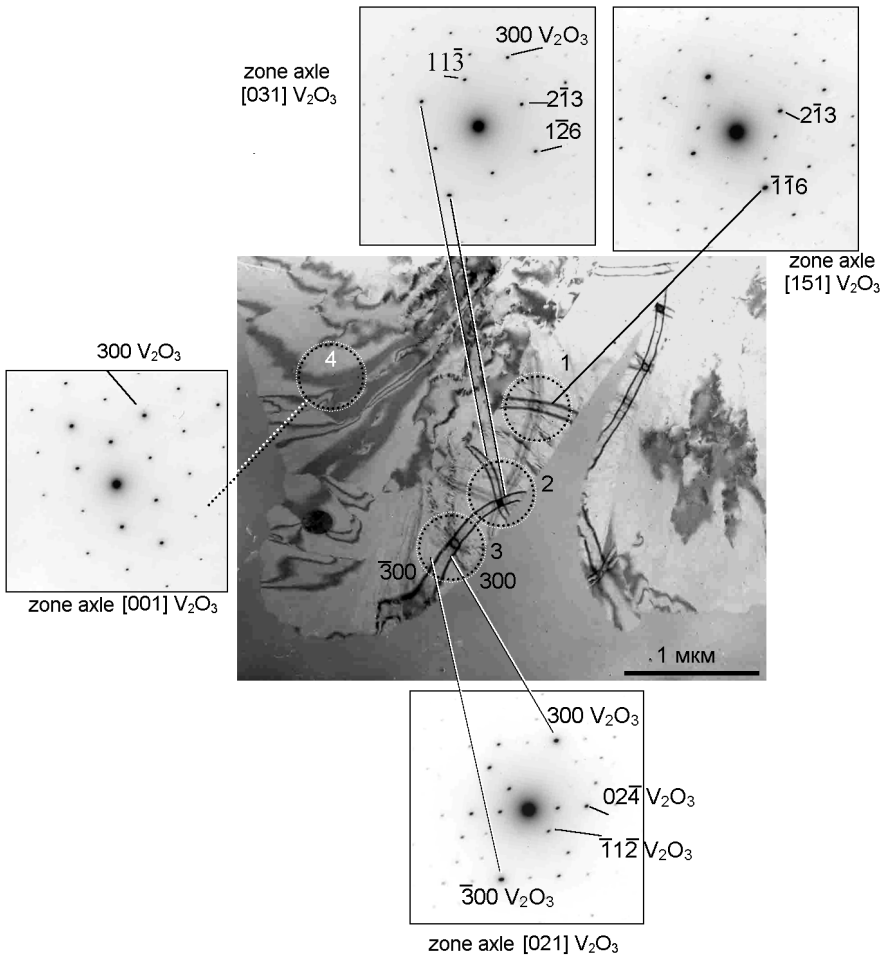

Fig. 4. The changes in zone-axial pictures (1–2–3) along a strip-like V_2O_3 crystal. The straight lines show the unambiguous connection between reflections (in electron diffraction patterns) and bend extinction contours (in the micrograph). The selected area of diffraction pattern from area 4 relates to the rounded crystal grown heterogeneously on a side surface of a strip-like one.

contours and of a varying zone axis pictures (1–2–3) in the image of a strip-like V_2O_3 crystal makes it possible to obtain the numerical characteristics of the crystal lattice bending using the formulas (1) and (2). The measured results are shown in the Table. According to this table, the curvature of the V_2O_3 crystal lattice attains ~42 deg/μm.

Thus, to conclude, at laser sputtering of vanadium in oxygen atmosphere, the capture of oxygen and its concentration C(O) in films at a fixed substrate temperature T_s grows with oxygen pressure $P(O_2)$ in the evaporation chamber whileat fixed $P(O_2)$, it decreases with increasing T_s. At $P(O_2) = 5 \cdot 10^{-3}$ Pa, within the T_s range from 20 up to 360°C, the crystal condensate $VO_{0.9}$ is formed. Above 190°C, the $VO_{0.9}$ film grows with a predominant (001)<110>$VO_{0.9}$//(001)<110>KCl orientation. At $P(O_2) = 1.3 \cdot 10^{-1}$ Pa, in the T_s range from 20 up to 200°C, the condensates containing amorphous (V_2O_3) and crystal ($VO_{0.9}$) components are formed. The fractionation of the film structure and phase composition depending on the condensation angle β of the vapor-plasma flow has been revealed. With growing β, the amorphous phase amount and oxygen contents in the film is increased. The crystallization of amorphous V_2O_3 phase is accompanied by increasing of the material density byt 9.2 %. The V_2O_3 spherulites growing in amorphous films have a curved crystal lattice. The value of its curvature attains 42 deg/μm.

This work has been done under the partial financial support by INTAS (Grant No.00-100).

Table. Characteristics of lattice bending in V_2O_3 crystal growing at crystallization of amorphous film (according to Fig. 4)

Zone number	Zone axis indices [u v w]	Integral lattice bending between zones i and k			Local lattice bending between contours (h k l) and ($\bar{h}$ $\bar{k}$ $\bar{l}$)		
		L^{ik} (μm)	φ^{ik}, deg	$\theta_{int}{}^{ik}$, (deg/μm)	(h k l)	Parameters of bending	
1	[1 5 1]	L_{12} = 0.52	14.5	27.9	1 1 $\bar{6}$	d(Å)	1.685
						W (μm)	0.043
						θ_{loc} (deg/μm)	29.3
					2 $\bar{1}$ 3	d(Å)	2.172
						W (μm)	0.050
						θ_{loc} (deg/μm)	19.52
2	031	L_{23} = 0.30	11.4	38.0	2 $\bar{1}$ 3	d(Å)	2.172
						W (μm)	0.047
						θ_{loc} (deg/μm)	20.77
					1 $\bar{2}$ 6	d(Å)	1.685
						W (μm)	0.032
						θ_{loc} (deg/μm)	39.32
					$\bar{1}$ $\bar{1}$ 3	d(Å)	2.172
						W (μm)	0.054
						θ_{loc} (deg/μm)	18.07
					$\bar{3}$ 0 0	d(Å)	1.420
						W (μm)	0.036
						θ_{loc} (deg/μm)	41.47
3	021	L_{31} = 0.80	24.3	30.4	$\bar{3}$ 0 0	d (Å)	1.420
						W (μm)	0.050
						θ_{loc} (deg/μm)	29.86

Note: L^{ik} is the distance between the centers of zone-axial patterns with zones directed to [u_i v_i w_i] and [u_k v_k w_k]. φ^{ik} is the angle between these zone axes. $\Theta_{int}{}^{ik}$ is a specific integral angle of crystal lattice turn between these zone axes; d, interplanar distance. W is the distance between pair of bend extinction contours. Θ_{loc} is the local specific angle of crystal lattice turn.

References

1. A.G.Bagmut, V.M.Kosevich, G.P.Nikolaichuk et al., *Functional Materials*, **6**, 75 (1999).
2. A.G.Bagmut, S.N.Grigorov, V.Yu.Kolosov et al., *Poverkhnost'*, No.11, 68 (2005).
3. R.N.Pletnyov, V.A.Gubanov, A.A.Fotiev, NMR in Vanadium Oxide Compounds, Nauka, Moscow (1979) [in Russian].
4. V.N.Andreev, M.A.Gurvich, V.A.Klimov et al., *Pis'ma v Zh.Tekhn.Fiz.*, **19**, 63 (1993).
5. R.A.Aliev, V.N.Andreev, V.A.Klimov et al., *Zh.Tekhn.Fiz.*, **75**, 81 (2005).
6. A.G.Bagmut, S.N.Grigorov, V.Yu.Kolosov et al., *Poverkhnost'*, No.10, 60 (2003).
7. V.Yu.Kolosov, A.R.Tholen, *Acta Materialia*, **48**, 1829 (2000).
8. International Center for Diffraction Data - JCPDC, 1996, card No.10-0313.
9. V.M.Ievlev, L.I.Trusov, V.A.Kholmyansky, Structure Transformations in Thin Films, Metallurgia, Moscow (1988) [in Russian].
10. P.Hirsch, A.Howie, R.Nicholson et al., Electron Microscopy of Thin Crystals, Butterworths, London (1965).
11. International Center for Diffraction Data - JCPDC, 1996, card No.26-0278.
12. A.V.Zenkevich, I.D.Khabelashvili, V.N.Nevolin, *Izv.VUZov: Elektronika*, No.2, 3 (1997).
13. B.K.Kotlyarchuk, L.G.Mansurov, G.V.Plyatsko et al., *Ukr.Fiz.Zh.*, **27**, 1066 (1982).

Структура та кристалізація лазерних конденсатів ванадію, осаджених в атмосфері кисню

О.Г.Багмут, С.М.Григоров, В.А.Жучков, В.Ю.Колосов, В.М.Косевич, Д.В.Мельніченко

Методами електронографії та просвічуваної електронної мікроскопії з використанням методик "in situ" і аналізу згінних екстинкціонних контурів діагностовано фазовий склад та структуру плівок, осаджених лазерним розпилюванням V в атмосфері кисню. Показано, що в інтервалі температур підкладки T_n (20–360°C) и тиску кисню у випаровувальній камері $P(O_2)$ ($5\cdot10^{-3}$–$1{,}3\cdot10^{-1}$ Па) при фіксованій T_n зміст кисню в плівках зростає з підвищенням $P(O_2)$, а при фіксованому $P(O_2)$ воно зменшується зі зростанням T_n. Встановлено області існування і склад кристалічної ($VO_{0,9}$) та аморфної (V_2O_3) фаз, а також ефект фракціонування складу плівки за кутом конденсації пароплазмового потоку. Сфероліти V_2O_3, що ростуть в аморфній плівці, мають зогнуту кристалічну решітку. Величина згину сягає ~42°/мкм. Кристалізація аморфної фази V_2O_3 супроводжується зростанням щільності на 9,2 %.